

Molecular Indicators of Surface and Bulk Instability of Hot Melt Extruded Amorphous Solid Dispersions

Ziyi Yang · Kathrin Nollenberger · Jessica Albers · Duncan Craig · Sheng Qi

Received: 30 July 2014 / Accepted: 12 September 2014 / Published online: 1 October 2014
© Springer Science+Business Media New York 2014

ABSTRACT

Purpose To identify molecular indicators of bulk and surface instabilities of amorphous dispersions prepared by hot melt extrusion.

Methods Four model drugs with different physicochemical properties were formulated with EUDRAGIT® E PO using hot melt extrusion. Samples were aged under a range of conditions for up to 6 months and characterized using SEM, ATR-FTIR, PXRD and MTDSC. The effects of a range of thermodynamic, kinetic and molecular parameters, including glass transition temperature, molecular mobility, the crystallization tendency of the amorphous drug and drug-polymer miscibility, on the bulk and surface stabilities of the solid dispersions were evaluated.

Results For all drug-containing systems, a higher degree of instability was observed at the surface of the material in comparison to the bulk. Stressed humidity showed a more profound effect on the dispersions in comparison to stress temperature, reducing both their surface and bulk stabilities. For supersaturated systems the order of the bulk and surface instabilities of the samples was found following the same order of the molecular mobilities of the amorphous model drugs. This was attributed to the presence of phase separation of amorphous drug-rich domains in the supersaturated extrudates.

Conclusions The stability of the amorphous drug-rich domains appears to be governed by the physical stabilities of the amorphous drugs. The more commonly used indicators such as T_g , fragility of the amorphous drug and the theoretically predicted drug-polymer solubility showed less influence on the bulk and

surface stabilities of the extrudates in comparison to the molecular mobility of the amorphous drug.

KEY WORDS amorphous molecular dispersions · hot melt extrusion · molecular mobility · physical stability · surface crystallization

INTRODUCTION

Amorphous molecular dispersions (also referred to as solid solutions) in which drugs are molecularly dispersed into polymeric carriers, have been reported to have better dissolution performance for delivering many poorly soluble drugs in comparison to solid dispersions containing crystalline drug (1,2). The transformation of drugs from the crystalline state to being in an amorphous molecular dispersion however often raises the concern regarding the increased physical instability of molecular dispersions (3–5). The physical stability of an amorphous molecular dispersion depends on a complex interplay between many factors, including the intrinsic properties of the drug and polymer and any drug-polymer interactions. The prediction and control of the physical stability of amorphous molecular dispersions still remain poorly understood as a result of a lack of knowledge of the key molecular

Electronic supplementary material The online version of this article (doi:10.1007/s11095-014-1527-8) contains supplementary material, which is available to authorized users.

Z. Yang · S. Qi (✉)
School of Pharmacy, University of East Anglia, Norwich, Norfolk, UK
NR4 7TJ
e-mail: sheng.qi@uea.ac.uk

Z. Yang · D. Craig
School of Pharmacy, University College London, 29-39 Brunswick
Square, London, UK WC1N 1AX

K. Nollenberger · J. Albers
Evonik Industries AG, Kirschenallee, Darmstadt, Germany

indicators that govern the physical stability of solid dispersions. Factors, such as drug-polymer solubility and miscibility, the glass transition temperature (T_g) and molecular mobility of amorphous systems and the storage conditions have all been linked to the physical stability of amorphous molecular dispersions (5–10). However in the past only the global bulk stability of a solid dispersion has been studied and the surface stability has been largely ignored. However, depending on the specific application of the solid dispersion, the surface stability can be much more important in affecting the *in vivo* performance of the formulation. Therefore it is important to gain a clear understanding of both bulk and surface stabilities of amorphous solid dispersions over a pharmaceutically relevant shelf-life.

Considering amorphous molecular dispersions using regular solution theory, a thermodynamically stable amorphous molecular dispersion requires the drug loading to be within the drug-polymer solid solubility at the storage temperature (10). The drug-polymer solubility therefore has become increasingly recognized as one of the most important thermodynamic factors influencing the tendency of phase separation and crystallization in amorphous molecular dispersions, although the methods used for the measurement of drug-polymer solubility are still being debated (11,12). However, in some cases dispersions with drug loading much higher than theoretically predicted solubility can still be kinetically stable over the typical pharmaceutical shelf-life (13). Therefore other factors also should be examined carefully in terms of their contribution to the physical instability of amorphous molecular dispersions.

The glass transition temperature is a physical feature of an amorphous system which is associated with molecular motion (6,14). With temperatures approaching T_g , the molecular motion of an amorphous system can increase substantially, which may lead to rapid drug crystallization. Therefore, the T_g s of amorphous drugs have been considered to be a key kinetic factor that can be correlated with the rate of drug crystallization (6). Besides the T_g , the intrinsic crystallization tendency of an amorphous drug has recently been reported as another important factor affecting the physical stability of amorphous molecular dispersions (15).

In this study, we used hot melt extrusion to prepare amorphous solid dispersions. This processing method has been increasingly attracting interest from formulation scientists for improving the dissolution performance of poorly water-soluble drugs (16–18). In many separate studies, the surface and bulk instabilities of HME extrudates have been reported (5,19–21). However, the factors governing the surface and bulk instabilities of HME dispersions have not been studied systematically. The principal aim of this study is to investigate the key molecular indicators influencing the surface and bulk physical instabilities of hot melt extruded amorphous molecular dispersions by evaluating thermodynamic, kinetic and

environmental factors. Four model drugs, felodipine, celecoxib, fenofibrate and carbamazepine with different physicochemical properties were selected to be formulated with a model polymer, EUDRAGIT® E PO. Thermodynamic factors including drug-polymer solubility and miscibility were evaluated using the melting point depression method (theoretical drug-polymer solubility) (7,22). Kinetic factors including the T_g and molecular mobility of the amorphous model drugs as well as the crystallization tendency of the amorphous model drugs alone were also studied. The influences of aging environments on the physical stability of amorphous molecular dispersions were also studied. The molecular mobility of the amorphous solid dispersions can be accelerated by increasing aging temperatures, possibly leading to crystallization (23). Increased humidity can lead to moisture uptake, resulting in the increased molecular mobility of drugs and decreasing stability of the dispersions (20).

MATERIALS AND METHODS

Materials

Felodipine, fenofibrate, celecoxib, carbamazepine and EUDRAGIT® EPO were kindly donated by Evonik Rohm Co.KG, Darmstadt Germany.

Preparation of Amorphous Drug

Amorphous drugs were prepared by two different methods, melt-cooling and spin coating, respectively. With regard to the melt-cool method, crystalline drugs were weighed in standard DSC pans. The DSC pans containing crystalline drugs were heated on top of a hot plate to a temperature 5°C above the melting point of the individual drug for 10 s. The samples were then removed from the hot plate and cooled under ambient conditions. Melt-cooled amorphous drugs were stored under both 0%RH/room temperature and 75%RH/room temperature, for up to 2 weeks.

Amorphous drugs were also prepared using spin coating. Before spin coating, crystalline drugs were individually dissolved in the mixture of ethanol and dichloromethane (50:50 v/v); the solid concentration of all drug solutions was 15% (w/v). A G3P-8 spin coater (Specialty Coating System, Surrey, UK) was used to prepare thin-film amorphous drugs from the model drug solutions. Thin films were spin coated on a microscope glass slide (25 mm × 25 mm). The spinning speed was set at 2,000 revolutions/min with a duration time of 2 min for the sample preparation in the spin coater. Spin coated amorphous drugs were also stored under 0%RH (provided by P₂O₅)/room temperature and 75%RH (provided by a saturated sodium chloride solution)/room temperature, for up to 2 weeks.

Hot Melt Extrusion (HME)

Hot melt extrusion was carried out using a Thermo Scientific HAAKE MiniLab II (Thermo Scientific, UK) with co-rotating twin screws. Crystalline drug and EUDRAGIT® EPO powders with ratios of 10:90 and 70:30 (w/w) were pre-mixed in a mortar and pestle before melt extrusion. The operation temperature was set at 5°C higher than the melting point of the individual drugs with a dwell time in the extruder of 5 min. The rotating speed of the screws was 100 revolutions/min. A round shape die with diameter of 2 mm was attached to the extruder. Moisture contents of all samples were tested using thermogravimetric analysis (TGA). All samples (including fresh and aged samples) had weight loss below 2% (w/w) after heated to 200°C.

Modulated Temperature Differential Scanning Calorimetry (MTDSC)

The modulated temperature differential scanning calorimetry (MTDSC) study was performed on a Q-2000 MTDSC (TA Instruments, Newcastle, USA). Temperature calibrations were carried out using standard materials with known melting points (T_m) including octadecane (T_m 28.24°C), indium (T_m 156.60°C) and tin (T_m 231.93°C). For modulated mode, the aluminium oxide sapphire was used for heat capacity calibration. The applied modulation parameters were $\pm 0.318^\circ\text{C}/60$ s with a $2^\circ\text{C}/\text{min}$ underlying heating rate. N_2 gas was used to purge through the DSC cell at a rate of 50 ml/min. TA standard crimped pans were used for all measurements. For each sample, triplicate measurements were performed ($n=3$).

Polarized Light Microscopy (PLM)

Polarised light microscopy studies were conducted using a Leica DM LS2 polarised light microscope (Wetzlar GmbH, Germany) connected to a video capture system. Spin coated samples were visualised under PLM with different magnification (specified in PLM images).

Powder X-Ray Diffraction (PXRD)

PXRD studies were carried out at room temperature with a Thermo-ARL Xtra diffractometer (Thermo scientific, UK). Strand form extrudates were milled by mortar and pestle before testing. Samples were placed on a zero background sample holder and attached onto a spinner stage. $\text{Cu K}\alpha_1$ with the wavelength of 1.54 \AA was used as the X-Ray source (voltage: 45 kV, current: 40 mA). The angular range ($3\text{--}80^\circ 2\theta$) was scanned with a step size of 0.01° and time per step of 0.5 s.

Attenuated Total Reflectance-Fourier Transform Infrared (ATR-FTIR) Spectroscopy

ATR-FTIR spectra of samples were collected on an IFS 66/S FTIR spectrometer (Bruker Optics Ltd, Coventry, UK) fitted with a Golden Gate® ATR accessory with heated top plate (Orpington, UK). The crystal used was a single reflection diamond element. The spectral resolution was 2 cm^{-1} , and 32 scans were taken for each sample. The surface and cross section of HME samples on aging were tested by ATR-FTIR spectroscopy. For isothermal studies, spectra were collected every 2 min.

Scanning Electron Microscopy (SEM)

The strand form samples and milled extrudates were sputter coated with Au/Pd. The images of the surface morphology of the samples were taken using a Phillips XL20 SEM (Phillips Electron Optics, Netherlands).

Kinetics of Surface Crystallization of HME Samples

In order to study the kinetics of the surface crystallization of HME samples on aging, image-analysis software, Image J (National Institutes of Health, USA), was used to track particle growth (in terms of surface area covered by the crystals) on the surface of HME samples on aging by analyzing SEM images taken at different time points. The size and shape of each individual particle was framed by the software, and the total areas occupied by particles in the whole SEM image were calculated.

Storage Conditions for HME Samples

Freshly prepared HME samples were stored as intact strand forms under four different conditions: 0%RH (provided by P_2O_5)/room temperature, 75%RH (provided by a saturated sodium chloride solution)/room temperature, 0%RH/40°C and 75%RH/40°C for up to 6 months.

RESULTS

Intrinsic Physical Stability of Amorphous Model Drugs

Physicochemical Properties of Amorphous Drugs

Physicochemical parameters including T_g and relaxation behavior of amorphous model drugs prepared by the melt-cool method are summarized in Table I. Details of the used methods for the calculation of the parameters have been well described in the literature and are provided in the

Table 1 Summary of the Physical Stability-Related Parameters of Four Model Drugs

Model drug	Felodipine	Celecoxib	Fenofibrate	Carbamazepine
T_g (°C) ($n=3$)	46.5	58.2	-19.7	50.1
Fragility index	52.58	106.05	56.77	116.71
Structural relaxation time at 25°C (s)	2.47×10^3	1.31×10^4	3.51×10^{-1}	1.78×10^3
Structural relaxation time at 40°C (s)	1.91×10^2	9.11×10^2	7.92×10^{-2}	2.63×10^2
Interaction parameter (miscibility) with EUDRAGIT® E PO	-1.03	-0.93	- ^a	-0.85
Solubility measured by melting point depression method (w/w)	30.7%(7)	41.1%	- ^a	45.1%

^a No melting point depression was detected

supplementary material (4,7,24–26). The results showed that the T_g s of the amorphous model drugs varied from -19.7 to 58.2°C. The broad range of T_g values allowed investigation of the link between the physical stability of molecular dispersions and the T_g of the drug. A fragility index study showed that felodipine and fenofibrate are strong glassy materials (index value below 100), whereas celecoxib and carbamazepine are weak glasses (index value above 100), indicating that the former two drugs are better glass-formers than the latter two drugs (27). The mean structural relaxation time of amorphous model drugs at different temperatures was calculated using the Adam-Gibbs-Vogel (AGV) equation with the achieved fragility index values (see supplementary material) (24). The mean structural relaxation time is a measure of the molecular mobility of amorphous materials at different temperatures and is the reciprocal of the molecular mobility (6). The impacts of molecular mobility on the stability and crystallization behavior of amorphous pharmaceuticals have increasingly been recognized (28). Therefore, by comparing with the real-time physical stability studies of HME samples, the relationship between the intrinsic thermodynamic properties of the amorphous drug and the physical stability of HME amorphous molecular dispersions can be evaluated.

Crystallization Tendency of Amorphous Model Drugs

The surface and bulk crystallization tendencies of amorphous drugs were explored under the conditions of 0%RH/room temperature and 75%RH/room temperature to match the aging conditions of HME samples. This allowed direct comparison of the crystallization tendency of amorphous drugs alone and the crystallization tendency of drug containing HME amorphous molecular dispersions. Surface crystallization tendencies of the amorphous model drugs were studied using thin-film amorphous drugs prepared by spin coating in order to maximize the surface to volume ratio and promote surface crystallization. Bulk crystallization tendencies of the amorphous model drugs were studied by MTDSC using the samples prepared in-situ in the DSC by melt-cool method. For the model drugs used in this study, the processing method

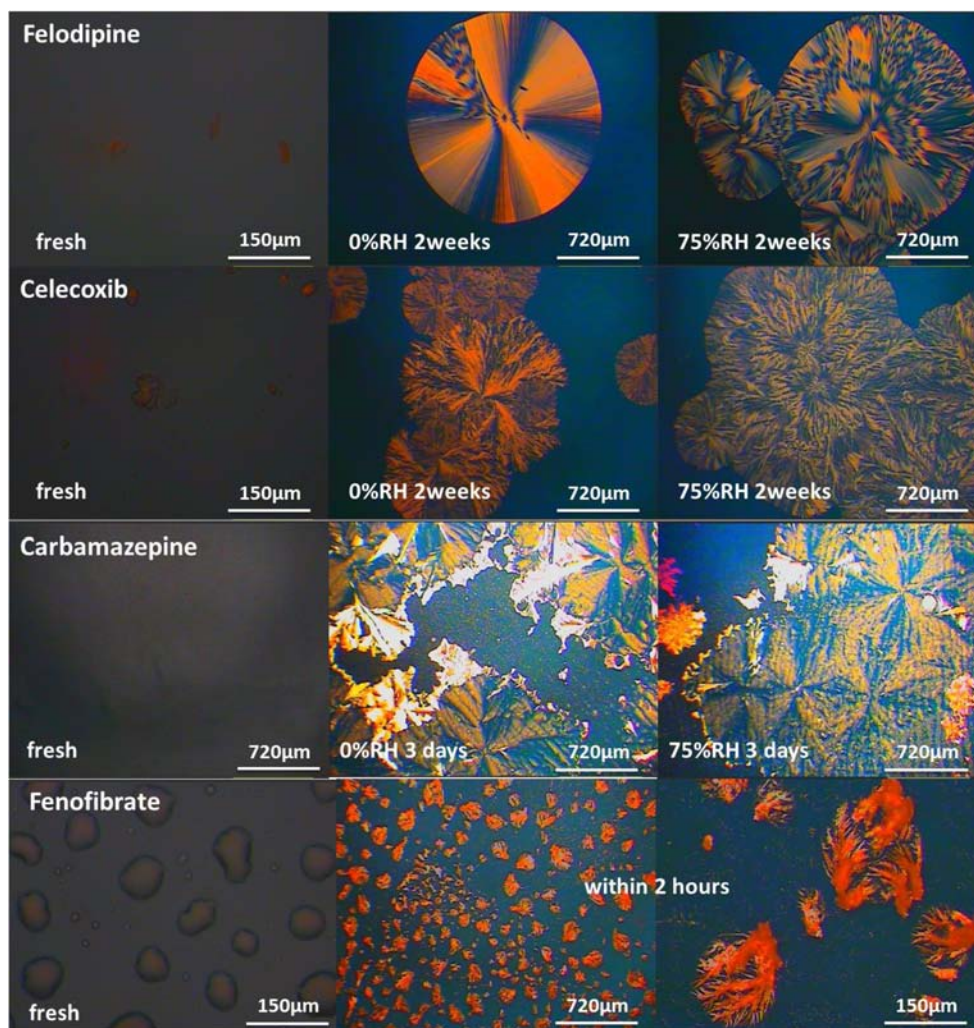
do not have significant impact on their crystallization behavior as reported in previous studies (29,30).

Surface Crystallization Behavior of Amorphous Model Drugs

PLM images of spin coated thin amorphous drug films aged under different conditions are shown in Fig. 1. No birefringence was observed in any freshly prepared spin coated model drug films, indicating all fresh samples were in amorphous state. After 2 weeks aging under 0%RH/room temperature, some crystalline domains were seen in spin coated felodipine and celecoxib. However the number of crystalline spherulites was lower for felodipine samples in comparison to celecoxib. A fast crystallization of spin coated amorphous carbamazepine aged under 0%RH/room temperature was confirmed by the presence of large crystalline domains after only 3 days aging. For spin coated amorphous fenofibrate at room temperature, no film was formed, but glassy droplets were observed on the glass substrate after spin coating. The ultra-fast surface crystallization of amorphous fenofibrate was demonstrated by the completion of surface crystallization within 2 h under ambient condition (23°C/50%RH). All spin coated amorphous samples were tested using ATR-FTIR spectroscopy (see supplementary material) which showed that after 2 weeks of aging, spin coated felodipine and celecoxib were still amorphous, indicating the observed crystallization is low in quantity; whereas within a relatively short aging time, crystalline carbamazepine (3 days) and fenofibrate (2 h) were detected by ATR-FTIR spectroscopy.

Under the condition of 75%RH/room temperature, the surface crystallization tendency of the amorphous model drugs remained the same order as the one observed under 0% RH (Fig. 1). However, a higher level of crystallization was observed in each individual amorphous model drug compared with the same sample aged under 0%RH/room temperature. For example, crystalline felodipine and celecoxib were also detected using ATR-FTIR spectroscopy after 2 weeks of aging under 75%RH/room temperature (see supplementary material), which indicates that surface crystallization rates of amorphous felodipine and celecoxib were accelerated by the stressed humidity. Overall the surface crystallization tendency of amorphous model drugs is felodipine \leq celecoxib < carbamazepine < fenofibrate.

Fig. 1 PLM images of the surfaces of the four spin coated amorphous model drugs aged under ambient temperature and different humidity (for fenofibrate samples the recrystallisation occurred within 2 h under ambient condition which is 23°C/50%RH).



Bulk Crystallization Behaviour of Amorphous Model Drugs. Bulk physical stabilities of amorphous model drugs were studied using melt-cooled samples. MTDSC results of amorphous model drugs after different aging periods and conditions are shown in Fig. 2. Fenofibrate recrystallizes rapidly after preparation, thus no further aging study was conducted. Under the aging condition of 0%RH/room temperature, no melting of crystalline felodipine on heating was detected after 2 weeks of aging, whereas crystallization followed by melting on heating in MTDSC was observed for amorphous celecoxib and carbamazepine after 1 day of aging. As for all three model drugs (felodipine, celecoxib and carbamazepine), their T_g can still be detected after 2 week aging, the melting enthalpies observed are likely to be largely contributed by the crystallization of amorphous celecoxib and carbamazepine during DSC heating. Although it can be concluded that amorphous celecoxib and carbamazepine are less stable on heating than amorphous felodipine, it is difficult to differentiate the bulk stabilities of the three at ambient temperature.

Under the condition of 75%RH/room temperature, crystalline felodipine was detected after 1 week aging, indicating crystallization of melt-cooled amorphous felodipine accelerated by stressed humidity. Crystallization on heating was observed for both melt-cooled celecoxib and carbamazepine. However, the crystallization exotherm occurred at lower temperatures with increasing the aging period in comparison to the samples aged under 0% RH. The high humidity may alter the nucleation process and subsequently affects the initiation of crystallization temperature (31). Nevertheless, the MTDSC results of melt-cooled amorphous model drugs still showed the order of bulk crystallization tendency was the same as the surface crystallization tendency, felodipine \leq celecoxib $<$ carbamazepine $<$ fenofibrate.

Drug-Polymer Miscibility and Solubility

Drug-polymer miscibility was estimated by calculating the interaction parameters between the model drugs and EUDRAGIT® E PO using the melting point depression method

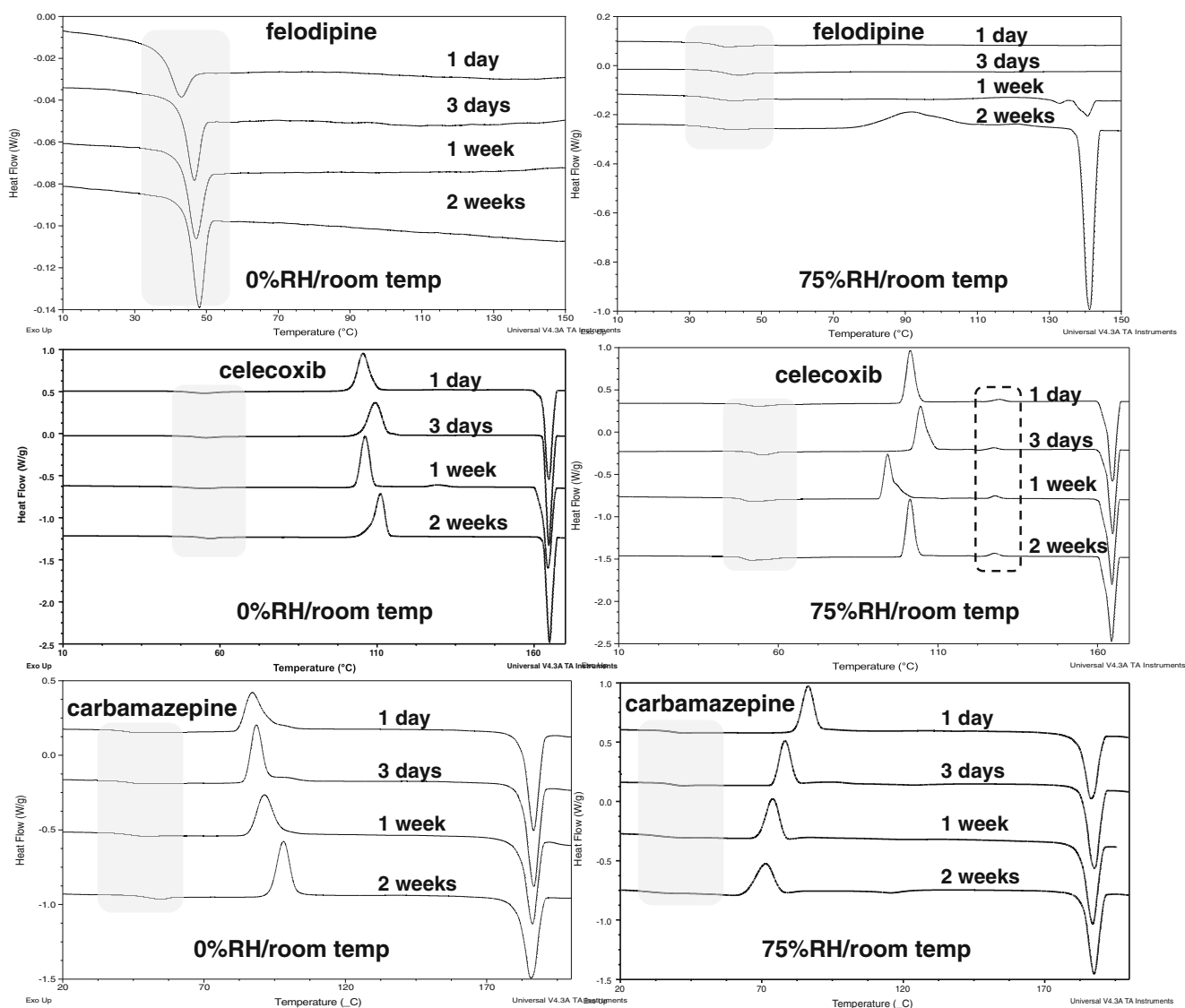


Fig. 2 MTDSC results of the bulk stability the amorphous drugs prepared by melt-cooling after different aging periods and conditions. (The grey areas highlight the glass transition regions of model drugs).

combined with Flory-Huggins lattice based theory (7,22,32). The detailed calculation for the model systems used in this study can be found in the [Supplementary material](#). As suggested by the method, negative interaction parameters suggest the drug and the polymer are miscible, whereas positive values indicate partial miscibility or that the drug and polymer are immiscible (7). Negative interaction parameters with EUDRAGIT[®] E PO were obtained for felodipine, celecoxib and carbamazepine, indicating that the three model drugs were miscible with EUDRAGIT[®] E PO at temperatures close to their melting points. The interaction parameter between fenofibrate and EUDRAGIT[®] E PO was not obtained due to the absence of depressed melting point in fenofibrate-EUDRAGIT[®] E PO physical mixtures even using the ultra-slow scanning rate of 0.2°C/min in the DSC measurement. This indicates poor miscibility between fenofibrate and

EUDRAGIT[®] E PO, which can be predicted from the absence of possible interaction functional groups within the molecular structures of fenofibrate and the polymer. The solid solubility of model drugs in the EUDRAGIT[®] E PO was calculated using the melting point depression method. It can be seen in [Table I](#) that the predicted solubility of felodipine, celecoxib and carbamazepine in EUDRAGIT[®] E PO are 30.7%, 41.1% and 45.1% (w/w), respectively. The solubility of fenofibrate in EUDRAGIT[®] E PO is unmeasurable using this method as indicated by the absence of melting point depression.

Real-Time Physical Stabilities of HME Extrudates

The T_g is a kinetic parameter for amorphous materials. It may affect crystallization of amorphous systems in that the

molecular motion of amorphous materials is increased substantially at temperatures approaching the T_g . Therefore if stored at room temperature, amorphous systems with higher T_g s may be more physically stable than those with low T_g s (6). The freshly prepared solid dispersion extrudates of EUDRAGIT[®] EPO with felodipine, celecoxib and carbamazepine were measured with T_g values above room temperature (in the range of 35–60°C) (Table II). The T_g values the extrudates with 10% and 70% fenofibrate are approximately 24.9 and –19.4°C, respectively. Both of these values are more than 10°C lower than the corresponding calculated T_g using Gordon-Taylor equation of the systems containing 10% and 70% fenofibrate. The DSC result of the 70% (w/w) fenofibrate extrudates, analyzed shortly after preparation showed a significant recrystallization peak on heating which may be contributed by the presence of significant amount of phase separated amorphous fenofibrate in the extrudates. Therefore solely judging from the T_g , the stability of the extrudates should follow the order of fenofibrate \leq carbamazepine < felodipine < celecoxib. Supersaturation (drug-loading higher than the solubility of drug in the carrier material) was one of the key thermodynamic driving forces of the physical instability of amorphous molecular dispersions. Therefore, the real-time physical surface and bulk stabilities of HME formulations with drug loadings below and above the predicted solubilities were studied and used to test the hypothesis.

Extrudates with Drug Loading Below the Predicted Saturate Solubility

Surface Instability. Real-time physical stability studies of HME samples showed that after 6 months aging under all conditions, no particles were observed on the surface of any 10% (w/w) felodipine-EUDRAGIT[®] E PO and celecoxib-EUDRAGIT[®] E PO samples in SEM images (see supplementary material). For 10% (w/w) carbamazepine, however, drug crystallisation was clearly observed on the surface of the samples after 6 month aging under all aging conditions, despite 10% is much lower than the predicted 45.1% solubility for carbamazepine in EUDRAGIT[®] E PO (Fig. 3). The 10% (w/w) fenofibrate-EUDRAGIT[®] E PO samples show a lower level of surface instability and a slower crystal growth rate than 10% (w/w) carbamazepine-EUDRAGIT[®] E PO samples (Fig. 4) after 6 months aging, even given the fact that the T_g of the fenofibrate dispersion is much lower than the carbamazepine loaded extrudates and the fenofibrate system is supersaturated according to the prediction from the melting point depression method (Table I). This demonstrates that T_g s of the model drug and the solid dispersion as well as the predicted solubility may not be the key parameters reflecting the physical stability of amorphous molecular dispersions.

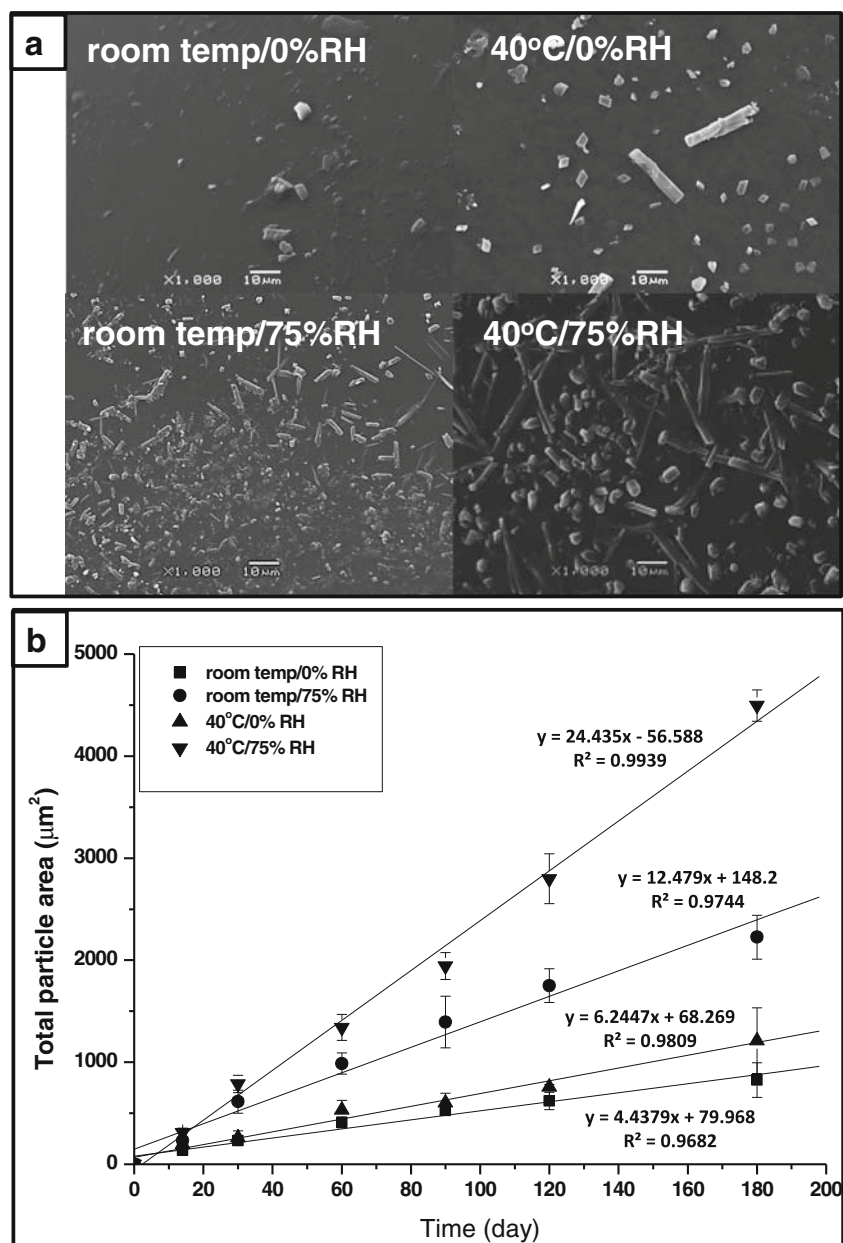
The surface crystallization kinetics of the 10% carbamazepine loaded extrudates was further studied by calculating the rate of coverage of the surface by the crystals during the course

Table II Summary of the Physical Stability Studies of Melt Extrudates Prepared with Model Drugs and EUDRAGIT[®] EPO Aged Under Different Conditions. ($n = 3$)

Model drug	Drug loading (%)	T_g (°C)		0%RH room temp	75%RH room temp	0%RH 40°C	75%RH 40°C
Felodipine	10%	45.4	Surface	A*	A	A	A
			Bulk	A	A	A	A
	70%	38.5	Surface ($\mu\text{m}^2/\text{day}$)*	10.3	33.3	11.6	172.9
			Bulk* (w/w)	0.27%	0.82%	0.45%	24.12%
Celecoxib	10%	53.5	Surface	A	A	A	A
			Bulk	A	A	A	A
	70%	60.1	Surface ($\mu\text{m}^2/\text{day}$)*	11.5	36.0	12.6	53.0
			Bulk	A	A	A	A
Fenofibrate	10%	24.9	Surface	A, C*	A, C	A, C	A, C
			Bulk	A	A	A	A
	70%	–19.4	Surface	fast recrystallization (completed within 200 min under ambient condition)			
			Bulk* (w/w)	57.43%	57.52%	58.02%	58.05%
Carbamazepine	10%	41.6	Surface ($\mu\text{m}^2/\text{day}$)*	4.4	12.5	6.2	24.4
			Bulk	A	A	A	A
	70%	28.4 ^x	Surface ($\mu\text{m}^2/\text{day}$)*	15.8	90.1	44.6	740.5
			Bulk	A	C	C	C

A*: amorphous solid dispersion; C*: crystalline drug; surface*: surface crystal growth rate; bulk*: crystallinity (w/w) in individual system after 6 months aging calculated the melt enthalpy of the drug; x: the 70% carbamazepine loaded extrudates may contain thermally degraded drug, thus the T_g is only used as an rough indicator

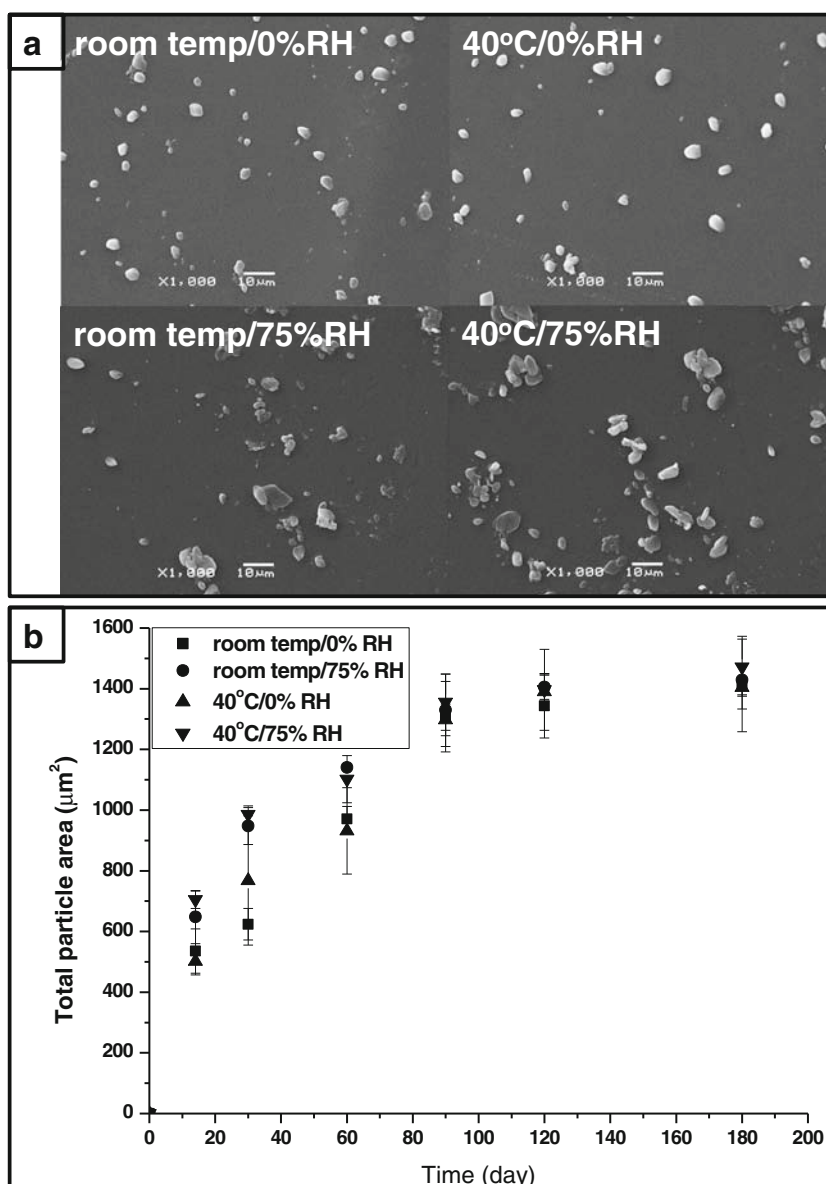
Fig. 3 Surface crystallization of 10% carbamazepine loaded aged HME solid dispersions. **(a)** SEM images of the surface of 6 months aged samples under different conditions; **(b)** kinetics of surface crystal growth on aging under different conditions.



of aging. The limitation of this image analysis based method is that it is not a direct quantitative method. Nevertheless it can provide indicative information on drug crystallization under different aging conditions for the purpose of comparison. It can be seen in Fig. 3b that carbamazepine had the highest rate of crystallization ($24.4 \mu\text{m}^2/\text{day}$) when the extrudates were aged under high humidity conditions (room temperature/75%RH and $40^\circ\text{C}/75\%RH$). Under 0%RH, the increase of aging temperature from ambient to 40°C shows little effect on the drug crystallization kinetics at the surface of the extrudates. However, the impact of storage temperature is dramatically magnified at 75%RH. The crystal growth rate at room temperature ($12.5 \mu\text{m}^2/\text{day}$) is half of the growth rate at 40°C under high humidity.

Surface recrystallization of carbamazepine was also confirmed using ATR-FTIR spectroscopy as shown in Fig. 5. The NH_2 group from amorphous carbamazepine in the freshly prepared 10% (w/w) melt extrudates was difficult to detect as a result of the low drug loading. After aging under 75%RH/room temperature for 2 months, a peak with a relatively high intensity at $3,464 \text{ cm}^{-1}$ was detected, which has the identical NH_2 peak position of that from crystalline form III carbamazepine, indicating, recrystallization into form III on aging under high humidity at room temperature (33,34). After 3 months aging under the same condition, another peak at $3,486 \text{ cm}^{-1}$ appeared and it was confirmed as form I crystalline carbamazepine (33,34), and thus

Fig. 4 Surface crystallization of 10% fenofibrate loaded aged HME solid dispersions. **(a)** SEM images of the surface of 6 months aged samples under different conditions; **(b)** kinetics of surface crystal growth on aging under different conditions.



amorphous carbamazepine on the surface of 10% (w/w) samples recrystallized into a mixture of form I and III under 75%RH/room temperature. Similar recrystallization occurred on the surface of 10% (w/w) samples aged under 75%RH/40°C, in which amorphous carbamazepine recrystallized into a mixture of form I and III. For 10% (w/w) melt extrudates aged under 0%RH/40°C, only form III carbamazepine was detected after 2 months storage. For 10% (w/w) samples aged under 0%RH/room temperature, no carbamazepine crystalline peaks were detected after 6 months storage. This is likely a result of the low quantity of the crystalline drug being below the detection limit of which instrument. Overall, the order of the surface instability of the under-saturated HME extrudates is carbamazepine < fenofibrate < felodipine ≤ celecoxib.

Bulk Instability. The bulk stability of the 10% drug loaded melt extrudates was studied using MTDSC (see [supplementary material](#)). After 6 months aging, no recrystallization or melting was detected by MTDSC in all 10% (w/w) extrudates with all four model drugs aged under all conditions, indicating high bulk physical stability of 10% (w/w) sample. It is recognized that the limits of detection of MTDSC may not be able to detect the trace amount of crystalline drug (if any present). However, it also indicates that if any crystalline drug present, the quantity is negligible. For 10% fenofibrate and carbamazepine loaded extrudates, this also suggests that the instability mainly occurred at the surfaces and the overall quantities of the recrystallized drug was negligible at a bulk level.

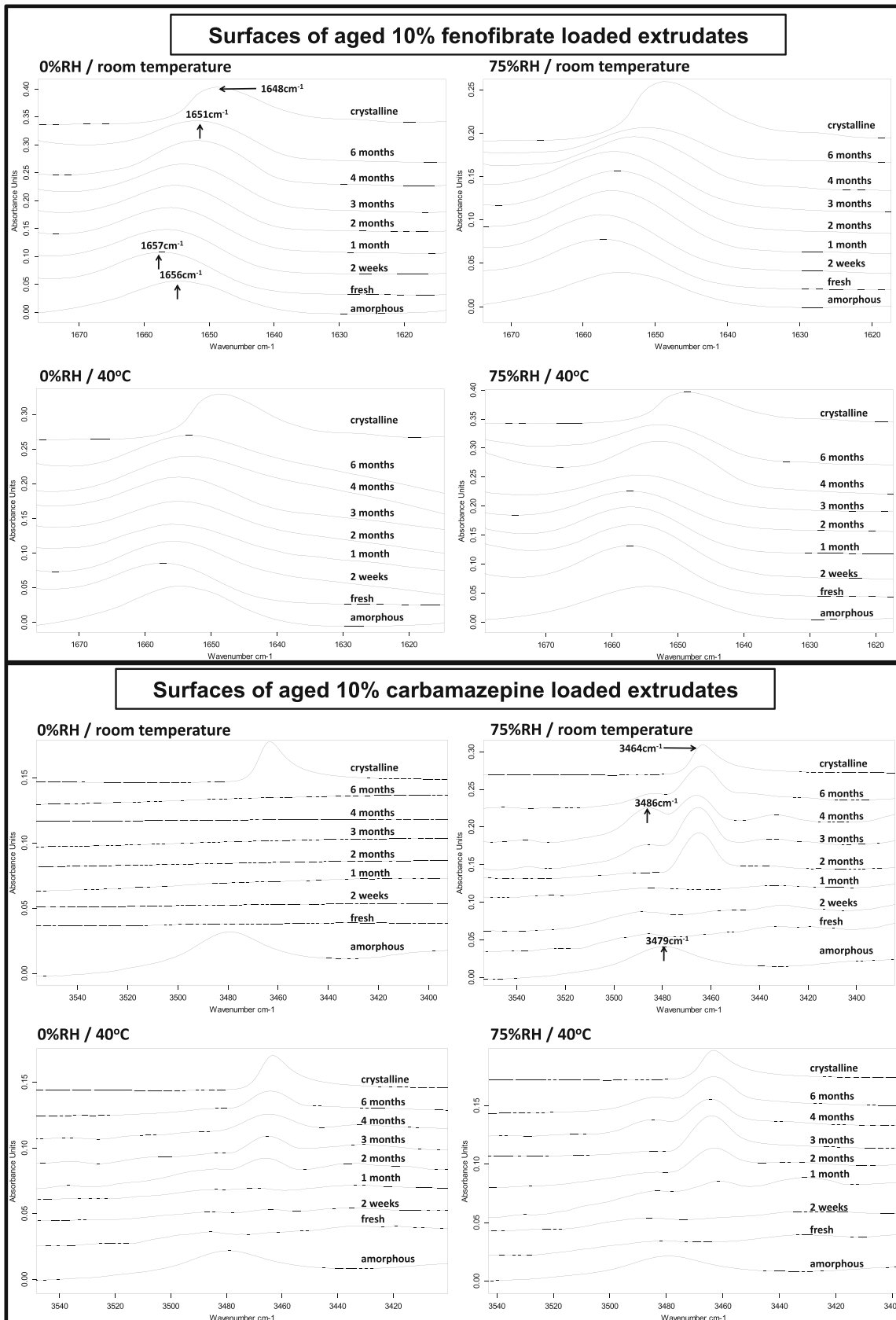


Fig. 5 Partial ATR-FTIR spectra of the surfaces of aged 10% fenofibrate and carbamazepine loaded HME amorphous molecular dispersions.

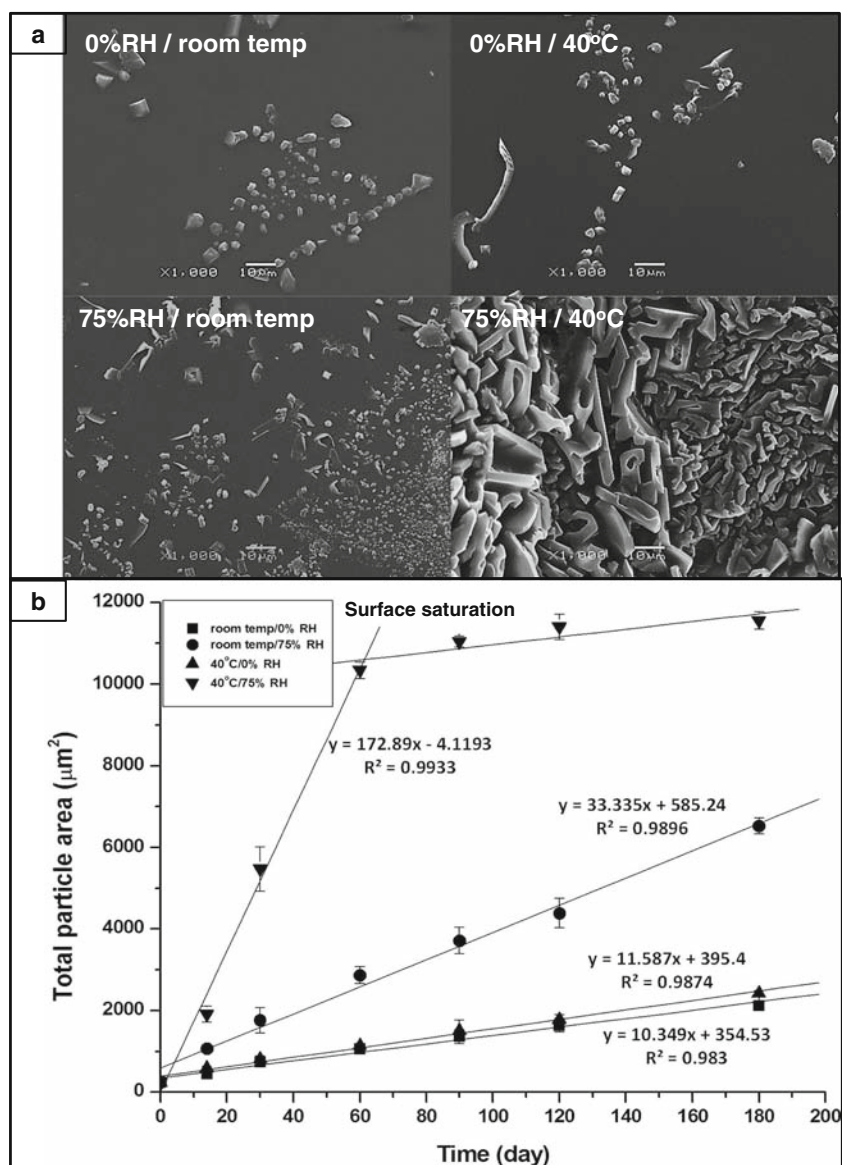
Extrudates with Drug Loading Above the Predicted Saturate Solubility

Surface Instability. Surface instability was detected in all 70% (w/w) HME felodipine-EUDRAGIT[®] EPO samples aged under different aging conditions, as shown in Fig. 6. For 70% (w/w) samples aged under all conditions, the kinetics of surface crystal growth all followed zero order. Surface crystallization did not follow the classic Avrami model with the sigmoidal pattern (35). This is likely due to the rapid recrystallisation shortly after the extrusion process. The samples aged at 75%RH/40°C exhibited fast crystallization kinetics (Fig. 6b). The surfaces of the extrudates were rapidly saturated (with a growth rate of 172.9 $\mu\text{m}^2/\text{day}$) by crystals within the first 2 months aging. With reducing the aging temperature to room temperature, the growth rate shows

nearly six-fold reduction. The absence of humidity leads to further two-fold reduction in crystal growth rate at the surface and temperature change has no significant impact on the growth kinetics.

Surface crystallization of 70% (w/w) felodipine-EUDRAGIT[®] E PO samples were also confirmed by ATR-FTIR study (Fig. 7). Aged under 75%RH, the NH peak from felodipine in the amorphous molecular dispersions ($3,341\text{ cm}^{-1}$) shifted to the peak position close to the NH peak from crystalline felodipine ($3,365\text{ cm}^{-1}$) after 1 week and 1 month for the samples aged under 40°C and room temperature, respectively. For samples aged under 0%RH, surface phase separation was also confirmed by the presence of both crystalline and amorphous felodipine NH peaks (Fig. 7). This co-existence of amorphous and crystalline felodipine occurred after 1 week and 2 weeks aging for the samples aged at 40°C

Fig. 6 Surface crystallization of 70% felodipine loaded aged HME solid dispersions. (a) SEM images of the surface of 6 months aged samples under different conditions; (b) kinetics of surface crystal growth on aging under different conditions.



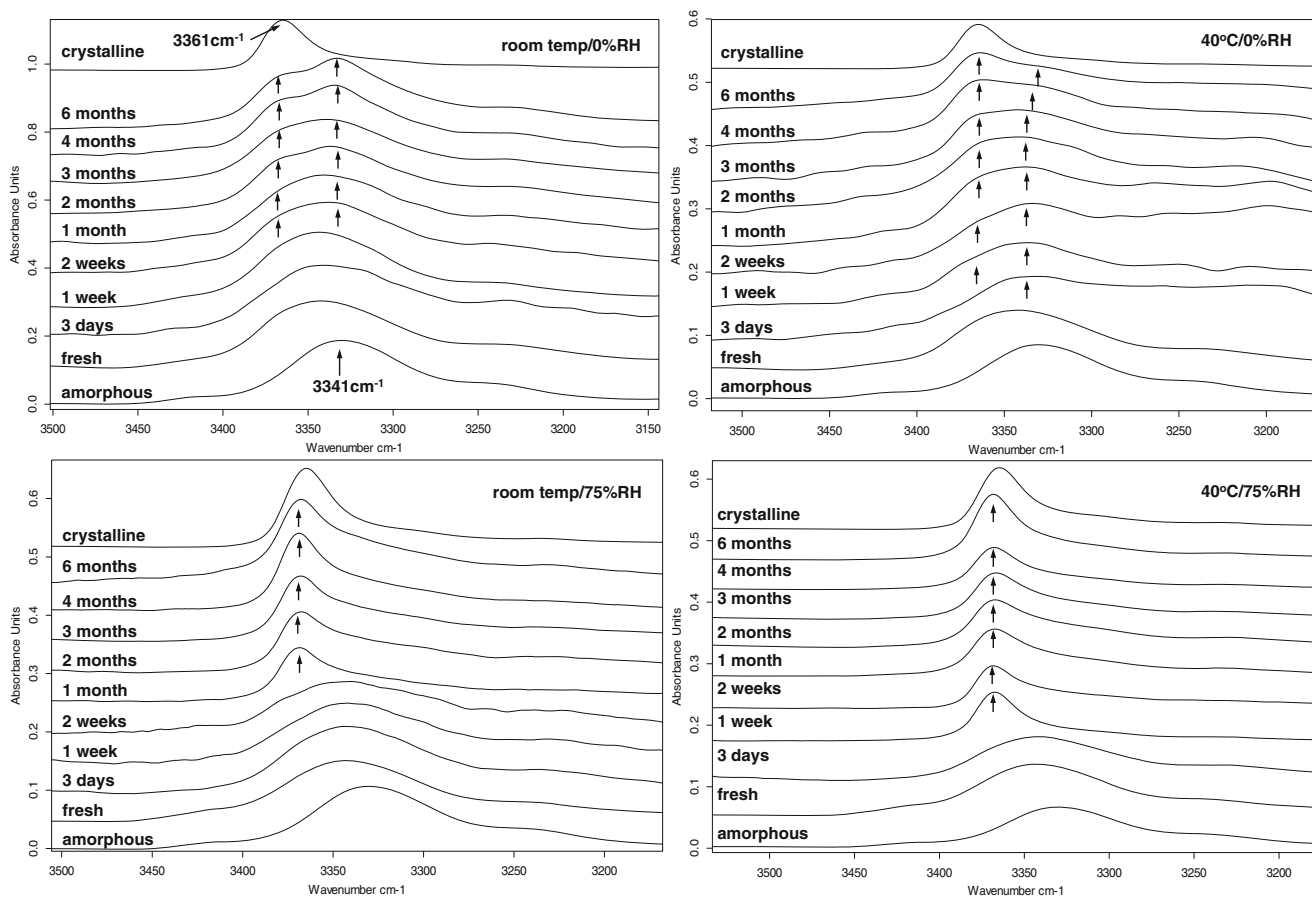


Fig. 7 Partial ATR-FTIR spectra (NH group) of the surface of aged 70% felodipine loaded HME amorphous molecular dispersions.

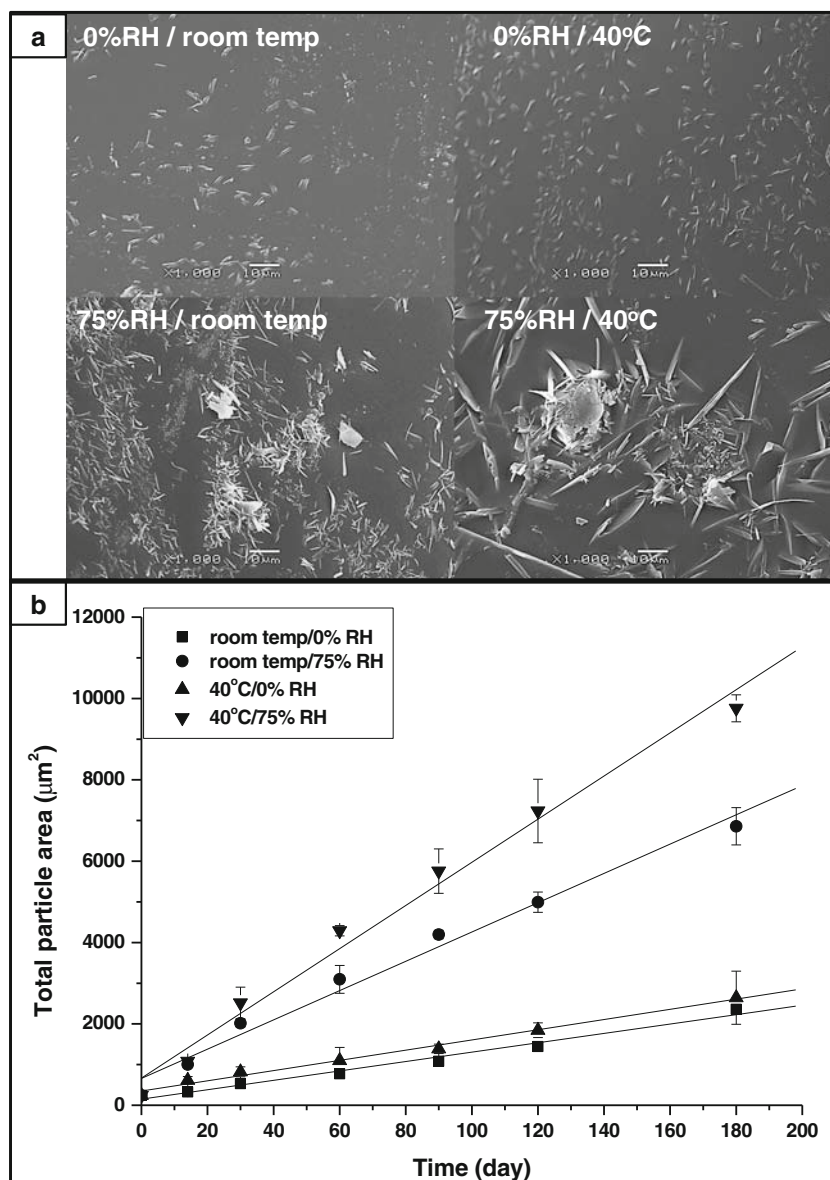
and room temperature, respectively. The sample aged at 40°C/0%RH also show high intensity of the crystalline phase peak in comparison to the samples aged at room temperature, indicating more crystallization under elevated aging temperature.

Figure 8 shows the surface crystallization in 70% (w/w) HME celecoxib-EUDRAGIT[®] E PO samples on aging under different conditions. Zero order crystal growth kinetics was observed for all 70% (w/w) samples aged under all conditions (Fig. 8b). It is noted that under 40°C/75%RH celecoxib shows much slower growth rate ($53.0 \mu\text{m}^2/\text{day}$) in comparison to the felodipine loaded extrudates aged under the same condition. For all other aging conditions, the growth rates of celecoxib are similar to the corresponding felodipine samples. The effect of humidity on the surface instability of celecoxib loaded extrudates is less than the one for felodipine loaded extrudates. Surface crystallization of 70% (w/w) celecoxib-EUDRAGIT[®] E PO samples were also confirmed using ATR-FTIR spectroscopy (Fig. 9). The SO_2 group from celecoxib was used to identify the physical state of celecoxib (36). For the 70% (w/w) samples aged under 75%RH/40°C, an additional peak of SO_2 group at $1,345 \text{ cm}^{-1}$ (crystalline celecoxib) was observed after 3 days aging, which proved the occurrence of surface crystallization on aging. The reduction of

the peak intensity of the amorphous peak at $1,338 \text{ cm}^{-1}$ with the progress of the aging indicates the continuous crystallization at the surface. The co-existence of both amorphous and crystalline peaks for the samples aged under different conditions suggests the presence of both amorphous celecoxib-rich domains and crystalline celecoxib at the surfaces of aged extrudates.

Lack of melting point depression for fenofibrate in EUDRAGIT[®] E PO indicates the immiscible nature of the system. Two super-saturation levels were studied for fenofibrate, low degree of super-saturation with 10% drug loading and high degree of super-saturation with 70% drug loading. For 10% fenofibrate loaded extrudates, the change of aging conditions shows no significant effect on the crystal growth rate at the surface of the extrudates (Fig. 4). A single carbonyl peak at $1,657 \text{ cm}^{-1}$, which is very close to the carbonyl peak ($1,656 \text{ cm}^{-1}$) from amorphous fenofibrate was detected on the surface of freshly prepared 10% (w/w) sample, suggesting an amorphous drug-polymer system on the surface of the freshly prepared samples. On aging under different conditions, this peak shifted progressively to $1,651 \text{ cm}^{-1}$ which is close to the carbonyl peak ($1,648 \text{ cm}^{-1}$) of crystalline fenofibrate. This gradual carbonyl peak shift indicates drug recrystallization on aging.

Fig. 8 Surface crystallization of 70% celecoxib loaded aged HME solid dispersions. **(a)** SEM images of the surface of 6 months aged samples under different conditions; **(b)** kinetics of surface crystal growth on aging under different conditions.



As the surface crystallization of 70% (w/w) HME fenofibrate-EUDRAGIT[®] E PO samples was rapid, it was monitored using ATR-FTIR spectroscopy immediately after preparation under ambient condition. As seen in Fig. 10a, freshly prepared 70% (w/w) samples were proved as amorphous by the position of the carbonyl group ($1,656\text{ cm}^{-1}$). Under the ambient condition, the amorphous drug carbonyl peak gradually shifted towards the crystalline drug carbonyl peak ($1,648\text{ cm}^{-1}$) within the timescale of less than 3 h, indicating rapid crystallization of the samples. The kinetics of the surface crystallization was further analyzed by monitoring the intensity ratio of the two peaks on the course of peak shifting (Fig. 10b). Three stages of surface crystallization were observed in the sample. Up to 160 min little change was seen in the spectra suggesting this stage being nucleation stage. The rapid crystal growth occurred between 160 and 360 min.

After 360 min, the growth rate dramatically reduced and slowly approached the completion of the crystallization.

Due to the possible minor thermal degradation of carbamazepine during the sample preparation in HME, the 70% (w/w) carbamazepine-EUDRAGIT[®] E PO extrudates may contain degradation product of the drug. Nevertheless the trend of surface crystallization was studied and shown in Fig. 11. It can be seen that the growth rate is much faster than the extrudates with 10% carbamazepine and the extrudates with 70% felodipine and celecoxib. High humidity (75%RH) conditions lead to significantly faster crystal growth rate (Fig. 11b). In contrast to the 10% systems, even under 0%RH elevated aging temperature dramatically increased the crystal growth rate at the surface of super-saturated extrudates. Comparing the surface crystallization behaviour of different formulations with 70% drug loading on aging

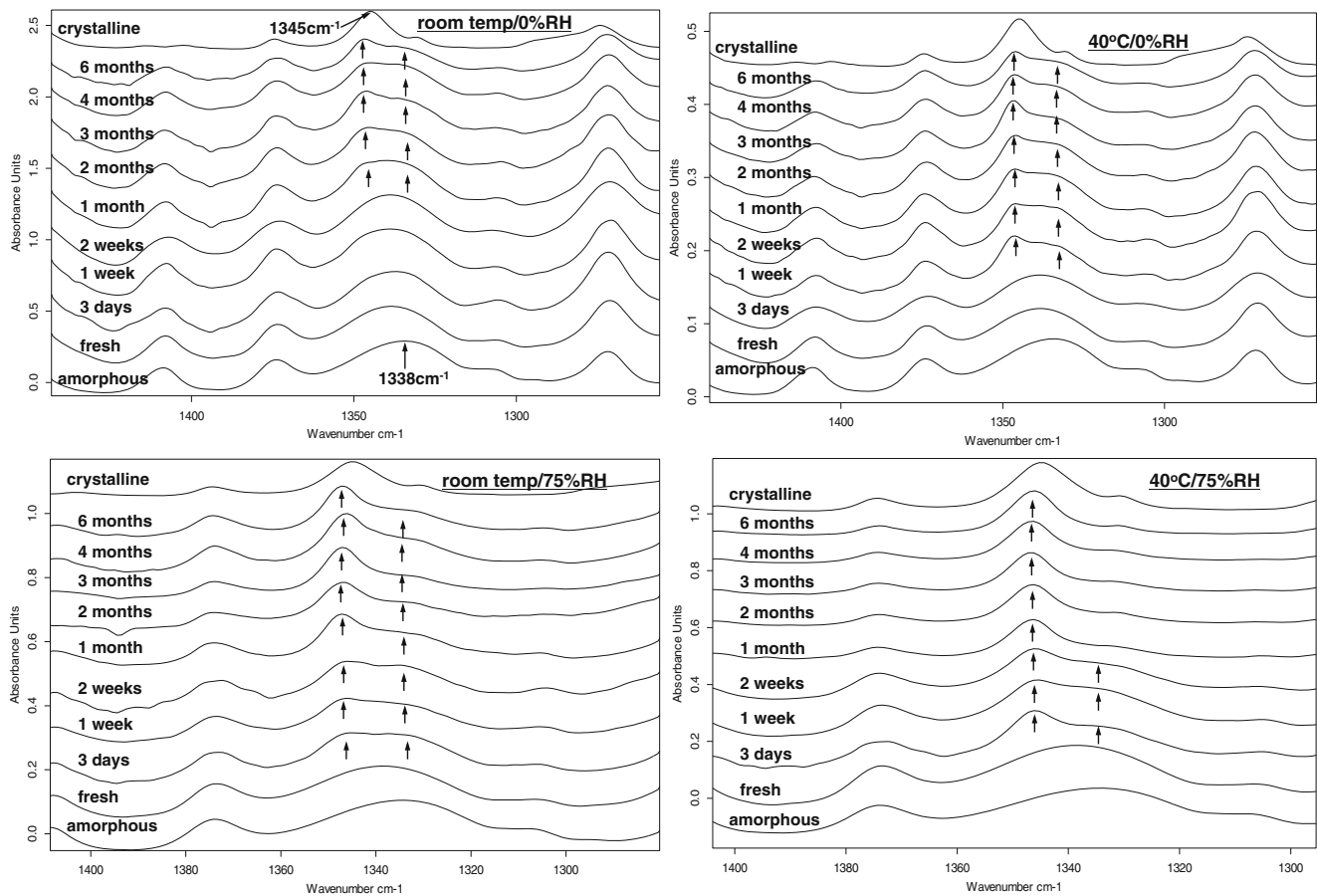


Fig. 9 Partial ATR-FTIR spectra of the surfaces of aged 70% celecoxib loaded HME amorphous molecular dispersions.

under different conditions, the order of the surface stability is celecoxib > felodipine > carbamazepine > fenofibrate.

Bulk Instability. In order to further quantify the crystallization in bulk, 70% (w/w) HME felodipine, celecoxib and carbamazepine-EUDRAGIT[®] E PO samples were tested using MTDSC and PXRD (Fig. 12). As no crystallization is observed on heating, the melting peak can be used as an

estimation of the crystalline drug in the sample. MTDSC results showed that after 6 months aging, the crystallinity in 70% felodipine-EUDRAGIT[®] E PO aged under 75%RH/40°C was estimated as 24% (w/w) (calculated using detected melting enthalpy in the sample divided by the melting enthalpy of pure crystalline felodipine). For the extrudates aged under other conditions, the crystallinity was all below 2% (w/w) detected by MTDSC and no crystallization was

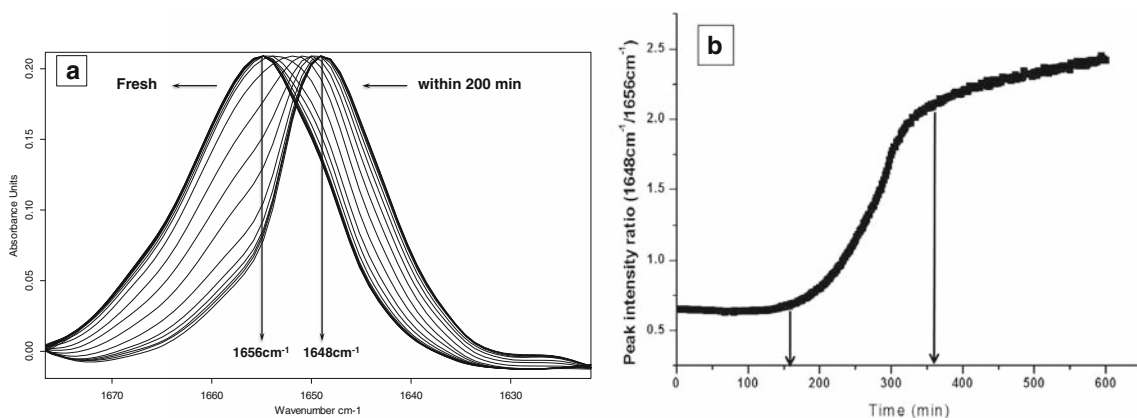
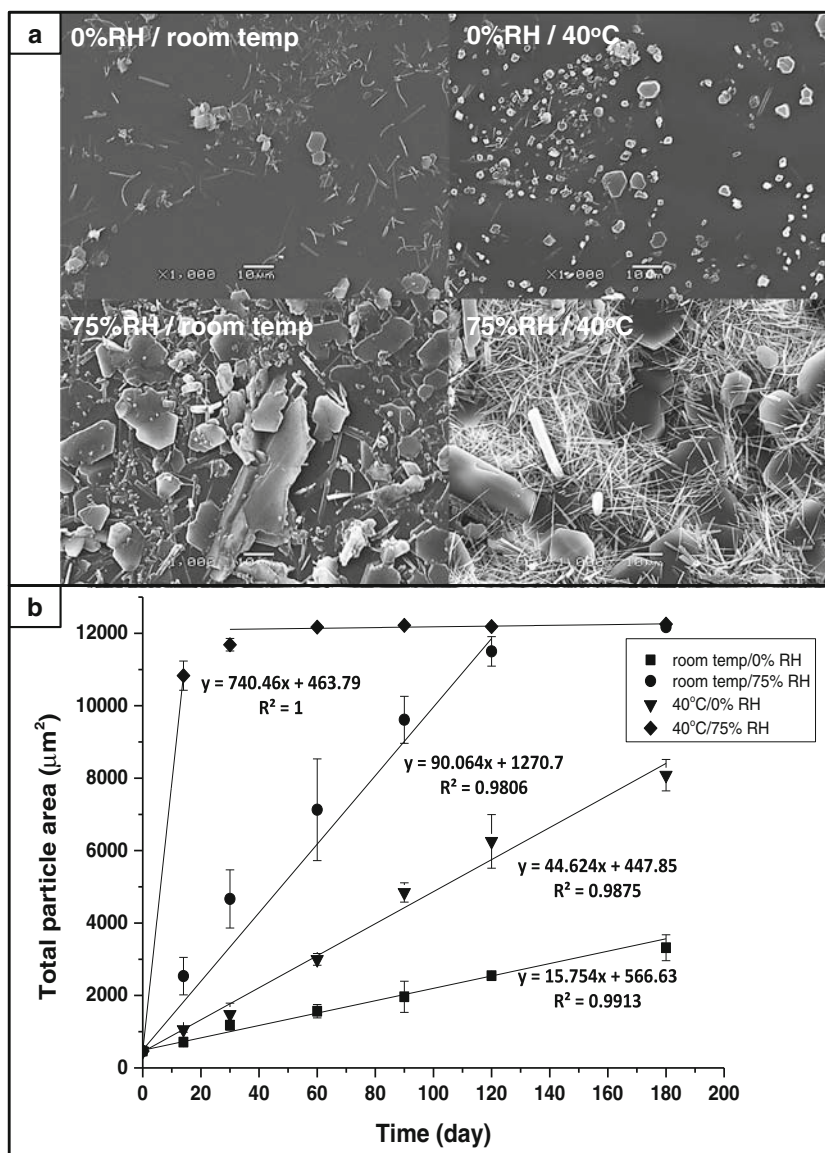


Fig. 10 Partial ATR-FTIR spectra of the surfaces of fresh 70% fenofibrate loaded HME amorphous molecular dispersions (a) and the change of the peak intensity ratio (b) under the ambient condition.

Fig. 11 Surface crystallization of 70% carbamazepine loaded aged HME solid dispersions. **(a)** SEM images of the surface of 6 months aged samples under different conditions; **(b)** kinetics of surface crystal growth on aging under different conditions.



detected at the cross section of these extrudates using ATR-FTIR spectroscopy. Therefore the detected melting of crystalline felodipine by MTDSC was likely to be contributed by surface crystallization. This was in agreement with the PXRD results (Fig. 12) that after 6 months aging, crystalline felodipine features was only detected in 70% (w/w) samples aged at 75%RH/40°C whereas samples aged under other conditions only showed amorphous halos in bulk. This indicates that despite the low surface stability, as bulk the polymer can stabilise supersaturated solid dispersion under the conditions with low humidity and low temperature.

70% (w/w) HME celecoxib-EUDRAGIT® E PO shows good bulk stability under all tested conditions within the tested period of 6 months. PXRD results (Fig. 12) show amorphous halos after 6 months aging under different conditions. DSC results show that crystallization

followed by melting was detected in fresh and all 6 months aged samples (Fig. 12). In this case, the melting enthalpy cannot be used to estimate the amount of crystalline drug in the aged extrudates as significant amount of crystalline drug was formed during DSC test. As no significant increase in the crystallization and melting enthalpy can be observed after aging (compared to the fresh samples), it can be concluded that the level of crystallization during aging is low. Phase separation of amorphous celecoxib-rich domains is evident in the samples aged under high humidity and elevated temperature. As seen in Fig. 12, the double T_g detected in the samples aged under 40°C and room temperature/75%RH indicates the presence of two types of amorphous phases, amorphous drug-rich phase and amorphous polymer-rich phase. It is also confirmed by the ART-FTIR results shown in Fig. 9.

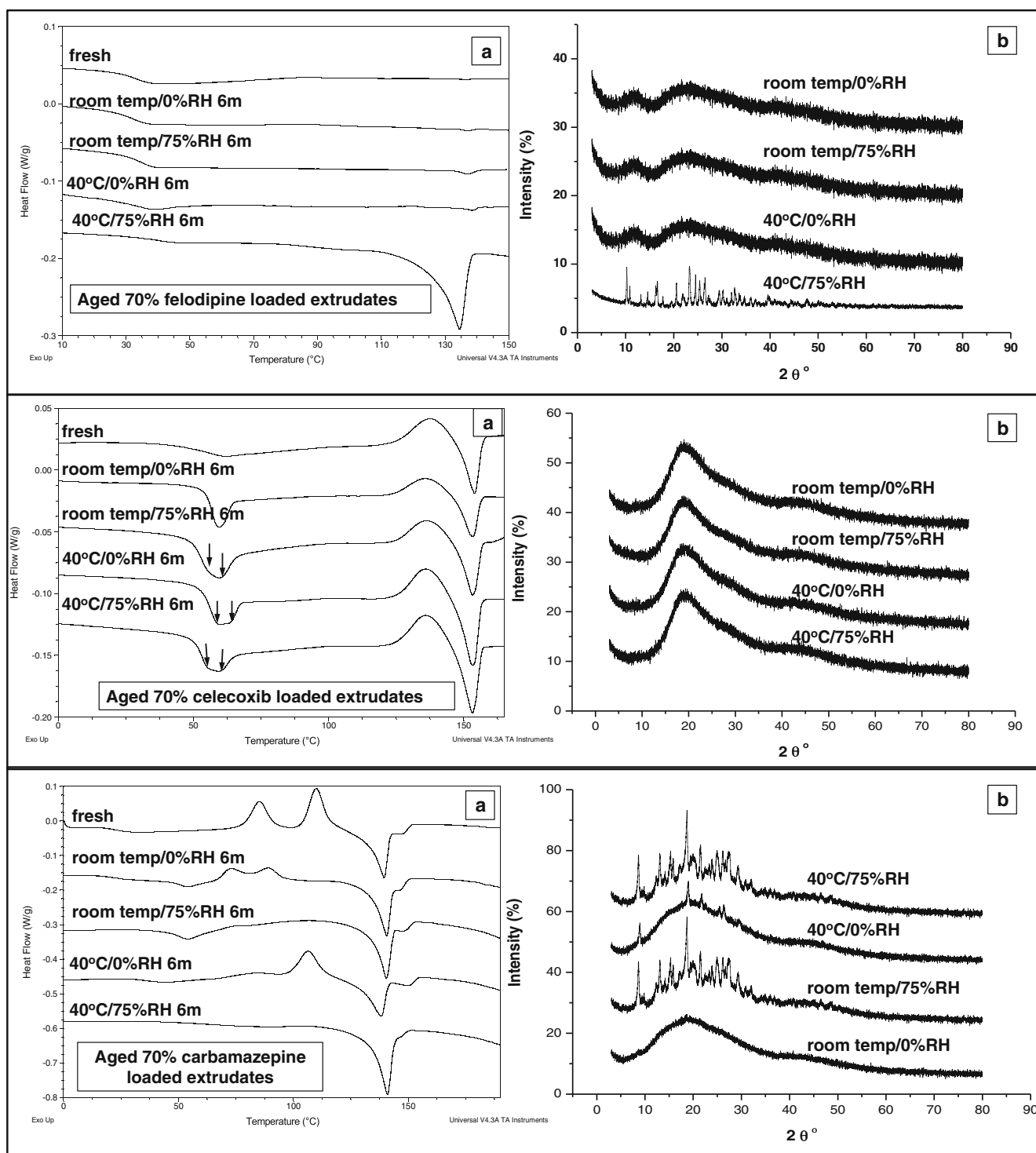


Fig. 12 Bulk stability of 6 months aged 70% (w/w) felodipine, celecoxib, and carbamazepine loaded HME amorphous molecular dispersions examined using (a) MTDSC and (b) PXRD.

Although degradation of the drug may present in the 70% carbamazepine loaded extrudates, the MTDSC and PXRD results on the bulk stability confirm the higher instability induced by high humidity condition than high temperature (Fig. 12). Under room temperature/0%RH, the 70% carbamazepine

loaded extrudates remain largely amorphous in bulk after 6 month aging despite the high surface instability observed.

For the extrudates with 70% fenofibrate tested shortly after the preparation, it is noted that an exothermic peak (recrystallization) was detected before melting, which indicates

crystallization of amorphous fenofibrate (Fig. 13). After 6 months aging under different conditions, the recrystallisation exotherm disappeared in the DSC results of the aged samples, indicating that most melting is contributed by the crystalline drug in the extrudates formed during aging. Therefore melting enthalpy was used to quantitatively estimate the fenofibrate crystallinity in the aged 70% (w/w) samples, which is approximately 58%. The T_g s detected in the DSC results of the aged samples matches the T_g of pure EUDRAGIT® E PO, indicating the possibility of the rest of 12% fenofibrate present as phase separate amorphous drug domains stabilised in the polymer matrix. This complete phase separation agrees well with the low miscibility and solubility prediction earlier. In summary, the trend of bulk stability of the supersaturated extrudates is in the same order as the surface stability being celecoxib > felodipine > carbamazepine > fenofibrate.

DISCUSSION

In this study, we attempted to reveal the origin of the physical instability of amorphous molecular dispersions prepared by hot melt extrusion through the analyses of thermodynamic, kinetic and environmental factors that can contribute to the surface and bulk instabilities. These include the intrinsic properties of the amorphous drug, such as T_g , fragility, molecular mobility and surface and bulk crystallization tendencies under different aging environments, the T_g of the amorphous solid dispersions and the miscibility and solubility of the drug in the polymer.

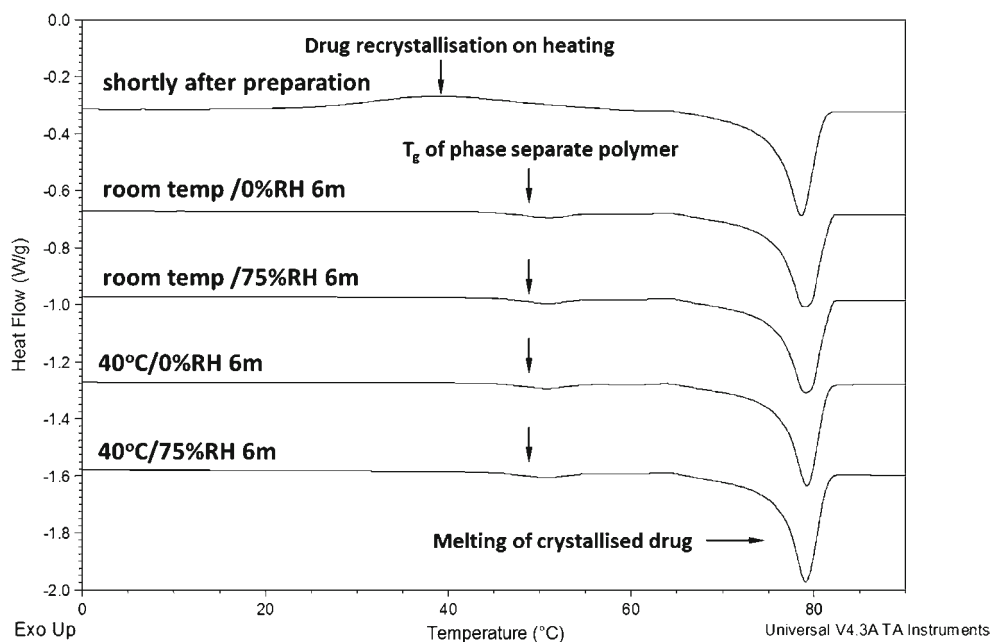
The results revealed the crystallization tendency of the amorphous drug alone follows the same trend of the

calculated relaxation time of the amorphous model drugs (Table I). However, T_g showed little use of accurately predicting the physical stability of the amorphous drug. The rate of surface crystallization is much faster than the bulk. High humidity has more profound effect on the drug crystallization than elevated aging temperature. The miscibilities and solubilities of the model drugs in the polymer are compatible for felodipine, celecoxib and carbamazepine. Fenofibrate was predicted to have poor miscibility and solubility with EUDRAGIT® E PO which can be partially attributed to the lack of intermolecular interaction between the drug and polymer.

For both under-saturated and supersaturated extrudates (in terms of drug loading below or above the predicted solubility), the development of surface instability is much faster than the bulk instability. This is due to the fact of the surface is the first interface of the bulk extrudates with the external environment. The higher surface energy, higher level of accumulation of moisture and sharper temperature gradient at the surface under stressed conditions and less steric constraint for crystal growth possibly leads to faster phase separation at the surfaces than in the bulk. Additionally, at the surface more heterogeneous nuclei are present and the non-constrained free upwards (out of the surface) crystal growth also is expected to lead to faster and higher level of instability at the surface than in the bulk.

Most under-saturated extrudates show low level of surface and bulk instability. However for under-saturated carbamazepine extrudates despite the predicted high miscibility and solubility of carbamazepine in EUDRAGIT® E PO, higher surface instability was observed in comparison to felodipine

Fig. 13 MTDSC results of 6 months aged 70% (w/w) fenofibrate loaded HME amorphous molecular dispersions.



and celecoxib. The reason of this is not clear, but carbamazepine has higher molecular mobility than felodipine and celecoxib (Table I). After comparing the data, it is clear that for super-saturated extrudates the surface and bulk instabilities are largely governed by the crystallization tendency and molecular mobility of the amorphous drug. High level of phase separation of amorphous drug-rich domains in the super-saturated extrudates leads to the exposure of amorphous drug-rich phases at the surfaces of the extrudates which crystallize on aging. As these domains follow the similar crystallization behavior as amorphous drug alone, the order of surface instability of super-saturated extrudates is same as the order of the molecular mobility of the amorphous drug. The responses of these samples to different environments also follow the same trend as the behavior of the amorphous drug alone.

In terms of the environmental factors, it was proven that stressed humidity had more impact on the physical stability, in particular surface stability, of solid dispersions than stressed temperature. This finding can be useful for the establishment of storage recommendations for amorphous molecular dispersions.

In summary, this study revealed that the significant link between the molecular mobility of the amorphous drug and the physical instability of hot-melt extruded amorphous molecular dispersions with drug loadings either below or above the solubility. Traditionally reported factors, such as T_g and the theoretically predicted drug-polymer solubility, showed less governing effect on the physical stability of the extrudates in comparison to the molecular mobility in this study. For the model drugs used in this study, high humidity exhibited much significant impact on both surface and bulk instabilities of the extrudates than elevated aging temperature. The findings of this study may contribute to the formulation development of hot-melt extruded amorphous molecular dispersions in respect of screening suitable drug candidates, selecting drug loadings and establishing storage conditions.

CONCLUSIONS

The physical stability, both at the surface and in bulk, of amorphous molecular dispersions prepared by hot melt extrusion can be affected by thermodynamic, kinetic and environmental factors. The results of this study confirmed the importance of molecular mobility of the amorphous drug on the physical stability of HME extrudates. The higher surface instability than the bulk for all studied systems highlighted the significance of surface instability. The governing effect of molecular mobility on the physical instability of the supersaturated solid dispersions was realized via the formation of amorphous drug-rich domains formed during phase separation in these systems. The findings of this study can contribute

to the development of a systematic tool for the formulation design of hot melt extruded amorphous molecular dispersions.

ACKNOWLEDGMENTS AND DISCLOSURES

Ziyi Yang would like to thank Evonik for the financial support for the period of his PhD. The authors also would like to acknowledge the contribution of members of the Interreg IV A project funded by the European Union.

REFERENCES

- Serajuddin ATM. Solid dispersion of poorly water-soluble drugs: early promises, subsequent problems, and recent breakthroughs. *J Pharm Sci.* 1999;88:1058–66.
- Leunerand C, Dressman J. Improving drug solubility for oral delivery using solid dispersions. *Eur J Pharm Biopharm.* 2000;50:47–60.
- Yu L. Amorphous pharmaceutical solids: preparation, characterization and stabilization. *Adv Drug Deliv Rev.* 2001;48:27–42.
- Qi S, Gryczke A, Belton P, Craig DQM. Characterisation of solid dispersions of paracetamol and EUDRAGIT® E prepared by hot-melt extrusion using thermal, microthermal and spectroscopic analysis. *Int J Pharm.* 2008;354:158–67.
- Qi S, Belton P, Nollenberger K, Clayden N, Reading M, Craig DM. Characterisation and prediction of phase separation in hot-melt extruded solid dispersions: a thermal. *Microscopic and NMR Relaxometry Study.* *Pharm Res.* 2010;27:1869–83.
- Hancock B, Shamblin S, Zografi G. Molecular mobility of amorphous pharmaceutical solids below their glass transition temperatures. *Pharm Res.* 1995;12:799–806.
- Marsac P, Shamblin S, Taylor L. Theoretical and practical approaches for prediction of drug–polymer miscibility and solubility. *Pharm Res.* 2006;23:2417–26.
- Marsac P, Li T, Taylor L. Estimation of drug–polymer miscibility and solubility in amorphous solid dispersions using experimentally determined interaction parameters. *Pharm Res.* 2009;26:139–51.
- Qi S, Craig DM. Detection of phase separation in hot melt extruded solid dispersion formulations global vs. localized characterization. *Am Pharm Rev.* 2010;13:68–74.
- Qian F, Huang J, Hussain MA. Drug–polymer solubility and miscibility: stability consideration and practical challenges in amorphous solid dispersion development. *J Pharm Sci.* 2010;99:2941–7.
- Rumondorand ACF, Taylor LS. Effect of polymer hygroscopicity on the phase behavior of amorphous solid dispersions in the presence of moisture. *Mol Pharm.* 2009;7:477–90.
- Mahieu A, Willart J-F, Dudognon E, Danède F, Descamps M. A new protocol to determine the solubility of drugs into polymer matrixes. *Mol Pharm.* 2012;10:560–6.
- Yang Z, Nollenberger K, Albers J, Qi S. Molecular implications of drug–polymer solubility in understanding the destabilization of solid dispersions by milling. *Mol Pharm.* 2014;11:2453–65.
- Hancockand BC, Zografi G. Characteristics and significance of the amorphous state in pharmaceutical systems. *J Pharm Sci.* 1997;86:1–12.
- Ng YC, Yang Z, McAuley WJ, Qi S. Stabilisation of amorphous drugs under high humidity using pharmaceutical thin films. *Eur J Pharm Biopharm.* 2013;84:555–65.
- Repka MA, Battu SK, Upadhye SB, Thumma S, Crowley MM, Zhang F, *et al.* Pharmaceutical applications of hot-melt extrusion: part II. *Drug Dev Ind Pharm.* 2007;33:1043–57.

17. Kalivoda A, Fischbach M, Kleinebudde P. Application of mixtures of polymeric carriers for dissolution enhancement of fenofibrate using hot-melt extrusion. *Int J Pharm.* 2012;429:58–68.
18. Maniruzzaman M, Rana MM, Boateng JS, Mitchell JC, Douroumis D. Dissolution enhancement of poorly water-soluble APIs processed by hot-melt extrusion using hydrophilic polymers. *Drug Dev Ind Pharm.* 2013;39:218–27.
19. Ke P, Hasegawa S, Al-Obaidi H, Buckton G. Investigation of preparation methods on surface/bulk structural relaxation and glass fragility of amorphous solid dispersions. *Int J Pharm.* 2012;422:170–8.
20. Qi S, Moffat JG, Yang Z. Early stage phase separation in pharmaceutical solid dispersion thin films under high humidity: improved spatial understanding using probe-based thermal and spectroscopic nanocharacterization methods. *Mol Pharm.* 2013;10:918–30.
21. Yang Z, Nollenberger K, Albers J, Moffat JG, Craig DQM, Qi S. The effect of processing on the surface physical stability of amorphous solid dispersions. *Eur J Pharm Biopharm.* 2014. Accepted.
22. Nishiand T, Wang TT. Melting point depression and kinetic effects of cooling on crystallization in poly(vinylidene fluoride)-poly(methyl methacrylate) mixtures. *Macromolecules.* 1975;8:909–15.
23. Andronisand V, Zografi G. The molecular mobility of supercooled amorphous indomethacin as a function of temperature and relative humidity. *Pharm Res.* 1998;15:835–42.
24. Yoshioka M, Hancock BC, Zografi G. Crystallization of indomethacin from the amorphous state below and above its glass transition temperature. *J Pharm Sci.* 1994;83:1700–5.
25. Qi S, Avalle P, Saklatvala R, Craig DQM. An investigation into the effects of thermal history on the crystallisation behaviour of amorphous paracetamol. *Eur J Pharm Biopharm.* 2008;69:364–71.
26. Zhou D, Zhang GGZ, Law D, Grant DJW, Schmitt EA. Thermodynamics, molecular mobility and crystallization kinetics of amorphous griseofulvin. *Mol Pharm.* 2008;5:927–36.
27. Hodge IM. Strong and fragile liquids — a brief critique. *J Non-Cryst Solids.* 1996;202:164–72.
28. Bhattacharyaand S, Suryanarayanan R. Local mobility in amorphous pharmaceuticals—characterization and implications on stability. *J Pharm Sci.* 2009;98:2935–53.
29. Baird JA, Van Eerdenbrugh B, Taylor LS. A classification system to assess the crystallization tendency of organic molecules from undercooled melts. *J Pharm Sci.* 2010;99:3787–806.
30. Van Eerdenbrugh B, Baird JA, Taylor LS. Crystallization tendency of active pharmaceutical ingredients following rapid solvent evaporation—classification and comparison with crystallization tendency from undercooled melts. *J Pharm Sci.* 2010;99:3826–38.
31. Surana R, Pyne A, Suryanarayanan R. Effect of aging on the physical properties of amorphous trehalose. *Pharm Res.* 2004;21:867–74.
32. Floryand PJ, Krigbaum WR. Thermodynamics of high polymer solutions. *Annu Rev Phys Chem.* 1951;2:383–402.
33. Rustichelli C, Gamberini G, Ferioli V, Gamberini MC, Ficarra R, Tommasini S. Solid-state study of polymorphic drugs: carbamazepine. *J Pharm Biomed Anal.* 2000;23:41–54.
34. Grzesiak AL, Lang M, Kim K, Matzger AJ. Comparison of the four anhydrous polymorphs of carbamazepine and the crystal structure of form I. *J Pharm Sci.* 2003;92:2260–71.
35. Avrami M. Kinetics of phase change. I General theory. *J Chem Phys.* 1939;7:1103–12.
36. Chawla G, Gupta P, Thilagavathi R, Chakraborti AK, Bansal AK. Characterization of solid-state forms of celecoxib. *Eur J Pharm Sci.* 2003;20:305–17.